J. Mod. Power Syst. Clean Energy (2019) 7(4):887–898
https://doi.org/10.1007/s40565-019-0533-6

μPMU-based smart adaptive protection scheme for microgrids

Mohamed Salah ELBANA[1], Nabil ABBASY[1], Ashraf MEGHED[1], Nahil SHAKER[1]

Abstract The concepts of microgrids (MGs) and smart grid represent the recent targeted revolution towards fully smart electrical network integrated with high penetration of renewable energy sources (RESs). The protection system of MGs becomes a challenge due to variable characteristics of its currents, bidirectional power flow and output power fluctuations of RES, causing selectivity and sensitivity issues for conventional protective devices (PDs) with fixed setting. In this paper, a smart protection scheme (SPS) is proposed using micro-phasor measurement units (μPMUs) to obtain the continuous rapid synchronized phasor measurement data. And it is communicated with a microgrid central controller (MGCC) through highly reliable communication architecture to carry out online smart adaptive protection scheme. Fault index coefficients and abnormality coefficients are calculated for each feeder to detect the fault location and the abnormality case. Detailed modeling of an MG including 10-bus connected distribution system with integrated distributed generation (DG) is simulated using ETAP software. The proposed protection algorithm is modeled and evaluated using MATLAB software. The proposed fault detector and abnormality detector can enable quick and accurate fault identification and isolation.

Keywords Fault index coefficients, Microgrid (MG), Micro-phasor measurement unit (μPMU), Renewable energy source (RES), Smart protection scheme (SPS)

CrossCheck date: 8 March 2019

Received: 19 November 2018 / Accepted: 8 March 2019 / Published online: 24 June 2019

✉ Mohamed Salah ELBANA
eng-mohamed.elbanna@alexu.edu.eg

Nabil ABBASY
nabil.abbasi@alexu.edu.eg

Ashraf MEGHED
megahed@ieee.org

Nahil SHAKER
nmahmoud.ces@gmail.com

[1] Electrical Engineering Department, Faculty of Engineering, Alexandria University, Lotfy El-Sied St., P.O. Elhadara, Alexandria 21544, Egypt

1 Introduction

In recent years, there is an extensive increase in electrical loads due to the tendency of the electrification of daily life which causes huge increase in sensitive and critical electrical loads. It becomes highly required to provide more generation capacities and efficient energy production, delivery and utilization due to the lack and non-renewability of fossil-fuels. Previous years, especially in 2015, there were massive breakthroughs on renewable energy discipline with largest global capacity additions [1, 2].

The integration of renewable energy source (RES) to electrical grid reveals the fact that distribution grids should be transformed from passive to active networks with more smartness, especially in distribution level [3]. Microgrids (MGs) are considered as the main building blocks of smart grid in which distributed generations (DGs) are integrated near to local loads. The implementation of MG concept has several advantages in both conventional low-voltage (LV) and medium-voltage (MV) grids [4].

MG protection is one of the major challenges due to the active MG network. The load flow varies during different operation modes and faults [5]. Distributed energy

resources (DERs) lead to the increase of short-circuit currents. However, power electronic interface used with RESs limits the fault current within 1.2–1.3 rated current [6]. The conventional overcurrent protection system does not recognize the fault during islanded operation mode since it lies on the long-time tripping of overcurrent relay characteristics curve [7]. For a better protection, the system needs to be smart and carries out online system protection with fast tracking online measurement. In [8], a survey is provided on MG protection issues defining three severe impacts on conventional overcurrent protective devices (PDs), causing failure to trip (sensitivity issue), unnecessary tripping (selectivity issue) as well as affecting power system reliability and reclosing issues after system transients. These impacts arise from various current characteristics during different operation modes (grid-connected or islanded), transients and faults of the system. These severe impacts require a more active protective scheme for system conversion.

Several MG protection schemes have been proposed. IEEE Std 1547-2003 proposes to disconnect all DGs during faults to limit its effect during fault condition [9]. This method suffers in high integration of DGs from system stability and voltage dips. The integration of external device strategy is one of the common proposed protection schemes as illustrated in [10]. Fault current limiter (FCL) is proposed to limit the fault current to be equal to that without DG. However, this method suffers under large penetration of DGs due to complex coordination between circuit breakers and the sizing for FCLs. Reference [11] introduces a voltage-based protection scheme based on measured DC components by *d-q* model transformation of measured values detecting in-zone and out-of-zone faults in case of high impedance faults and reduced fault current. Fault analysis is reliable as it does not depend on MG current. But without depending on time tagged measurements, the un-synchronization between voltage components leads to data overlapping and false tripping. In [12], a current differential protection scheme is proposed, as it is not sensitive to bidirectional power flow. It measures three phase currents. The zero and negative sequence components were able to detect the earth fault, while the instantaneous phase current can be measured using the current transformer (CT). However, faults with high fault current containing a significant DC component lead to the saturation in the secondary winding of a CT, which results in maloperation. In [13], a microprocessor-based relay is proposed for LV MG. A line impedance protection scheme is proposed in [14], and it depends on measured feeder impedance with characteristics of inverse relay tripping. An adaptive protection scheme in LV MG is proposed in [15].

Communication system is a vital part of smart protection scheme (SPS), as any communication failure or communications signal distortion can lead to consequences that threaten the protection system reliability. It should be reliable and secure for transmitting measured data between several devices [16]. An MG central controller (MGCC) is expandable on SPS for future extension [17]. In case of communication failures, MGCC carries out dynamic state estimation to compute missed data due to this failure or to tune bad data detected.

In this paper, a new SPS for LV and MV networks is proposed. Micro-phasor measurement units (μPMUs) are used for online time tagged synchronized measurements aiding for fast control and optimal operation. A μPMU is now feasible to be used on LV grids, as it provides full system observability and high measurement accuracy [18, 19]. The algorithm relies on the μPMU in transferring synchronized measured phasors to MGCC to calculate fault index (D-index) for detecting of all types of short-circuit faults as well as abnormality coefficient ∂ to detect overload, over and under voltage condition. On fault or abnormal cases, faulted feeder is identified and based on pre-programmed action look-up table. A tripping command is issued for PDs on selective manner. The algorithm proves to solve all mentioned protection issues.

The paper is structured as follows: Section 2 introduces the proposed protection scheme including the communication system and controller. Section 3 illustrates the power system model. Section 4 represents the simulation results and discussions. Finally, Section 5 sums it all up.

2 Proposed protection scheme

A proposed SPS is developed to detect faults in LV and MV underground cables and transmission lines, in the case of grid-connected mode or islanded mode. Synchronized measurement from μPMUs optimally locates at certain buses for large-scale MGs or at both ends of feeders for small and rural MGs. The algorithm relies on travelling wave theory, using Clarke transformation to obtain the propagation time constant and fault coefficient index and relies on synchronized measurements for abnormality detection.

2.1 Fault detection

An MGCC carries out Clarke transformation to decouple the phase components of voltage and current signals into the modal waves that are released during fault occurrence [20, 21]. Clarke transformations of voltage and current signals are calculated by (1) and (2), respectively.

$$\begin{bmatrix} \boldsymbol{V}_a \\ \boldsymbol{V}_b \\ \boldsymbol{V}_c \end{bmatrix} = \boldsymbol{T} \begin{bmatrix} \boldsymbol{V}_0 \\ \boldsymbol{V}_\alpha \\ \boldsymbol{V}_\beta \end{bmatrix} \tag{1}$$

$$\begin{bmatrix} \boldsymbol{I}_a \\ \boldsymbol{I}_b \\ \boldsymbol{I}_c \end{bmatrix} = \boldsymbol{T} \begin{bmatrix} \boldsymbol{I}_0 \\ \boldsymbol{I}_\alpha \\ \boldsymbol{I}_\beta \end{bmatrix} \tag{2}$$

where V_a, V_b, V_c are time stamped 3-ϕ synchronized voltage phasors; I_a, I_b, I_c are the time stamped 3-ϕ synchronized current phasors; 0, α, and β are the Clark components of the 3-ϕ voltage and current. The Clark transformation matrix $\boldsymbol{T}$ is defined by:

$$\boldsymbol{T} = \frac{1}{\sqrt{3}} \begin{bmatrix} 1 & 2 & 0 \\ 1 & \frac{-1}{\sqrt{2}} & \frac{\sqrt{3}}{2} \\ 1 & \frac{-1}{\sqrt{2}} & \frac{-\sqrt{3}}{2} \end{bmatrix} \tag{3}$$

A modal propagation constant $\boldsymbol{\Gamma}$ is given by:

$$\boldsymbol{\Gamma} = \sqrt{\boldsymbol{T}^{-1}\boldsymbol{Z}\boldsymbol{Y}\boldsymbol{T}} \tag{4}$$

where $\boldsymbol{Z}$ and $\boldsymbol{Y}$ are line impedance and admittance matrices respectively. The characteristic impedance $\boldsymbol{Z_c}$ of the feeder is calculated based on (5), where V_{Am}, V_{Bm}, I_{Am}, I_{Bm} are the Clarke components at the sending and receiving end buses A and B, respectively. The entries of fault index vector $\boldsymbol{D}$ are determined by (6).

$$Z_c(i) = \frac{V_{Am}^2 - V_{Bm}^2}{I_{Am}^2 - {I_{Bm}}^2} \tag{5}$$

$$D(i) = \frac{\ln A(i) - C(i)/E(i) - B(i)}{2\Gamma(i,i)L} \quad i = 0, \alpha, \beta \tag{6}$$

where $A(i)$, $B(i)$, $C(i)$, and $E(i)$ are entries of 3×1 vectors defined by (7)–(10).

$$A(i) = \frac{V_{Bm}(i) + Z_c(i)I_{Bm}(i)}{2} \tag{7}$$

$$B(i) = \frac{V_{Bm}(i) - Z_c(i)I_{Bm}(i)}{2} \tag{8}$$

$$C(i) = \frac{V_{Am}(i) + Z_c(i)I_{Am}(i)}{2\mathrm{e}^{\Gamma(i,i)L}} \tag{9}$$

$$E(i) = \frac{V_{Am}(i) - Z_c(i)I_{Am}(i)}{2\mathrm{e}^{\Gamma(i,i)L}} \tag{10}$$

The full derivation of (4)–(10) can be found in [20].

2.2 Protection algorithm

Figure 1 shows the flowchart of SPS. A μPMU at each end of a feeder sends synchronized phasors to MGCC to carry out the Clarke transformation. MGCC carries out online parameter estimation to define the feeder characteristic impedance $\boldsymbol{Z_c}$. The magnitude of fault coefficient index D_{ij} is the fault detector for SC faults. If the magnitude of any component of D-index converges to exist instantaneously, the feeder is considered as the faulted

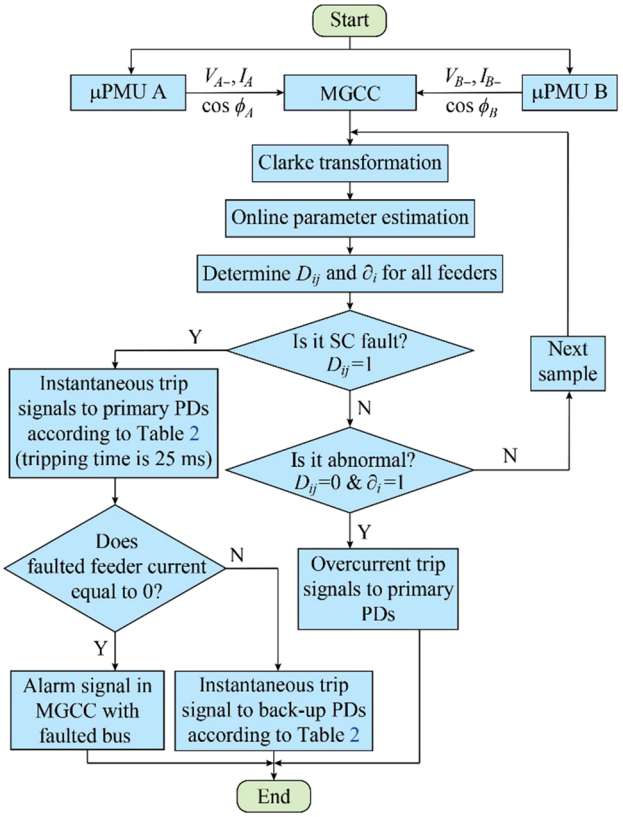

Fig. 1 Flowchart of proposed protection algorithm

Table 1 Event look-up table

D_{ij}	∂_i	Event
0	0	Normal operation
0	1	Abnormal case (overload, overvoltage, undervoltage)
1	0	SC fault case
1	1	Fault and abnormal case

feeder. If it tends to infinity, the feeder is healthy. Abnormality coefficient ∂_i of each bus is calculated in MGCC. If the overloading factor O_i equals to or is greater than 1, or if bus overvoltage coefficient O_v is greater than 1.15, or if bus under voltage coefficient U_v is less than 0.85, the MGCC sets logic values for the previous set of conditions. If the condition is satisfied, its logic value is set to be 1; if not, its value is set to be 0. The logic values of D_{ij} and ∂_i in terms of their component logic values are set as:

$$D_{ij} = D_0 + D_\alpha + D_\beta \tag{11}$$

$$\partial_i = O_i + O_v + U_v \tag{12}$$

For proper coordination, to isolate the smallest possible part of the MG, the proposed protection scheme selects the local PDs as per the event and action look-up tables built in

MGCC as shown in Table 1 and Table 2. Each MG has its selective look-up action table and event discrimination table. The table shows the programmed look-up action for the studied MG. In Tables 2, 1 means that a PD is normally operating; 0 means that PD is in a trip state; and 1' means that PD is on but is energized to trip a primary PD in case of failure.

2.3 Communication system

Fiber optical network is proposed to be implemented for transmitting data from μPMUs to MGCC and for sending signals from MGCC to PDs that contains tripping and operating decision based on calculated settings. It is based on real time communication. For reliable and secured data transmission from μPMUs to MGCC, a reliable GPS clock is required. The GPS signal and μPMU communication protocol must comply with IEEE C37.118 synchro-phasor standard. The proposed scheme is based on centralized communication architecture through MGCC that receives data from μPMUs and transmits decisions to local PDs.

2.4 Measurement and PDs

Each bus has its own μPMU due to the low cost and size of it compared with commercial PMUs. It provides the instantaneous measurement data of voltage and current signals to carry out the protection algorithm within 25 ms, as illustrated in the proposed protection algorithm section.

High-speed fast acting LV circuit breaker (LVCB) is proposed to be used as a protective device (PD) for proper instantaneous tripping time [22]. Also, the concept of fast silicon controller rectifier (SCR) based solid state switches which can trip within 8–17 ms and an insulated-gate bipolar transistor (IGBT) based switches can trip in faster manners [23] are better solutions to be used as the PDs to maintain a smart and fast communication through fiber optic cables. The tripping time of the protective scheme is within 25 ms based on the usage of real-time P-type half cycle μPMUs [24] with high phasor estimation accuracy. Both PMUs and μPMUs proves their validity on failure detection and cyber security applications [25].

Table 2 Event and action look-up table

Event	Signal																
	PD 1	PD 1.1, PD 2.1	PD 1.2, PD 7.1	PD 2	PD 2.2, PD 3.1	PD 3	PD 3.2, PD 4.1	PD 4	PD 4.2, PD 5.2	PD 5	PD 6	PD 5.1, PD 6.2	PD 6.1, PD 7.2	PD 7	PD 8	PD 8.1, PD 10	PD 8.2, PD 9
$D_{1\text{-}2}+\partial_{1\text{-}2}=1$ (LV microgrid internal fault feeder 1-2)	1'	0	1'	1'	1'	1	1	1	1	1	1	1	1	1	1	1	1
$D_{2\text{-}3}+\partial_{2\text{-}3}=1$ (LV microgrid internal fault feeder 2-3)	1	1'	1	1'	0	1'	1'	1	1	1	1	1	1	1	1	1	1
$D_{3\text{-}4}+\partial_{3\text{-}4}=1$ (LV microgrid internal fault feeder 3-4)	1	1	1	1	1'	1'	0	1'	1'	1	1	1	1	1	1	1	1
$D_{4\text{-}5}+\partial_{4\text{-}5}=1$ (LV microgrid internal fault feeder 4-5)	1	1	1	1	1	1	1'	1'	0	1'	1	1'	1	1	1	1	1
$D_{5\text{-}6}+\partial_{5\text{-}6}=1$ (LV microgrid internal fault feeder 5-6)	1	1	1	1	1	1	1	1	1'	1'	1'	0	1'	1	1	1	1
$D_{6\text{-}7}+\partial_{6\text{-}7}=1$ (LV microgrid internal fault feeder 6-7)	1	1	1'	1	1	1	1	1	1	1	1'	1'	0	1'	1	1	1
$D_{7\text{-}1}+\partial_{7\text{-}1}=1$ (LV microgrid internal fault feeder 7-1)	1'	1'	0	1	1	1	1	1	1	1	1	1	1'	1'	1	1	1
$D_{1\text{-}TR}+\partial_{1\text{-}TR}=1$ (LV microgrid external fault feeder 1-TR)	0	0	0	1'	1'	1	1	1	1	1	1	1	1'	1'	0	1	1
$D_{8\text{-}TR}+\partial_{8\text{-}TR}=1$ (MV microgrid external fault feeder 8-TR)	0	1'	1'	1	1	1	1	1	1	1	1	1	1	1	0	1'	1'
$D_{8\text{-}9}+\partial_{8\text{-}9}=1$ (MV microgrid external fault feeder 8-9)	1'	1	1	1	1	1	1	1	1	1	1	1	1	1	1'	1'	0
$D_{8\text{-}10}+\partial_{8\text{-}10}=1$ (MV microgrid external fault feeder 8-10)	1'	1	1	1	1	1	1	1	1	1	1	1	1	1	1'	0	1'

Note: represents primary PD trip signal; represents back-up PD; represents normal operated PD

STATE GRID
STATE GRID ELECTRIC POWER RESEARCH INSTITUTE

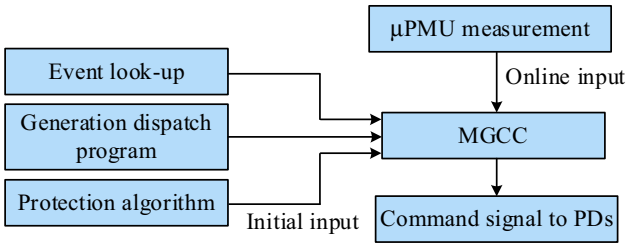

Fig. 2 Operational function of MGCC

2.5 MGCC

The function of MGCC is to take the decision of tripping and the operation of PDs. It is carried out by a station computer located in a secondary distribution substation as illustrated in Fig. 2. The look-up table can be programmed through simple software as to be applicable for each future extension.

3 Power system model

The proposed MG model includes both MV and LV loads. Inverter based photovoltaic (PV) DGs are integrated into the system model. The simulated MG is connected to MV utility, and its voltage level is 6.6 kV at a frequency of 50 Hz. Single line diagram of the power system model is shown in Fig. 3. It is simulated using ETAP software version 12.6.0 [26].

The system is operating in both grid-connected mode and islanded mode. It consists of 10 buses and includes MV synchronous motor as an industrial load and residential LV loads. The system parameters are given in Appendix A.

4 Simulation results

In this section, the proposed protection scheme will be evaluated in the power system model presented in the previous section. Several fault types are applied in different operation modes. The following are different case studies.

Case 1: normal operation in grid-connected mode with PV cells fully loaded, and micro-generators OFF.
Case 2: 3-ϕ fault in grid-connected mode with PV cells fully loaded, and micro-generators ON.
Case 3: 3-ϕ fault in islanded mode with PV cells fully loaded, and micro-generators OFF.
Case 4: 3-ϕ fault on islanded mode with PV cells OFF, and micro-generators ON.
Case 5: L-G fault in islanded mode with PV cells fully loaded, and micro-generators OFF.

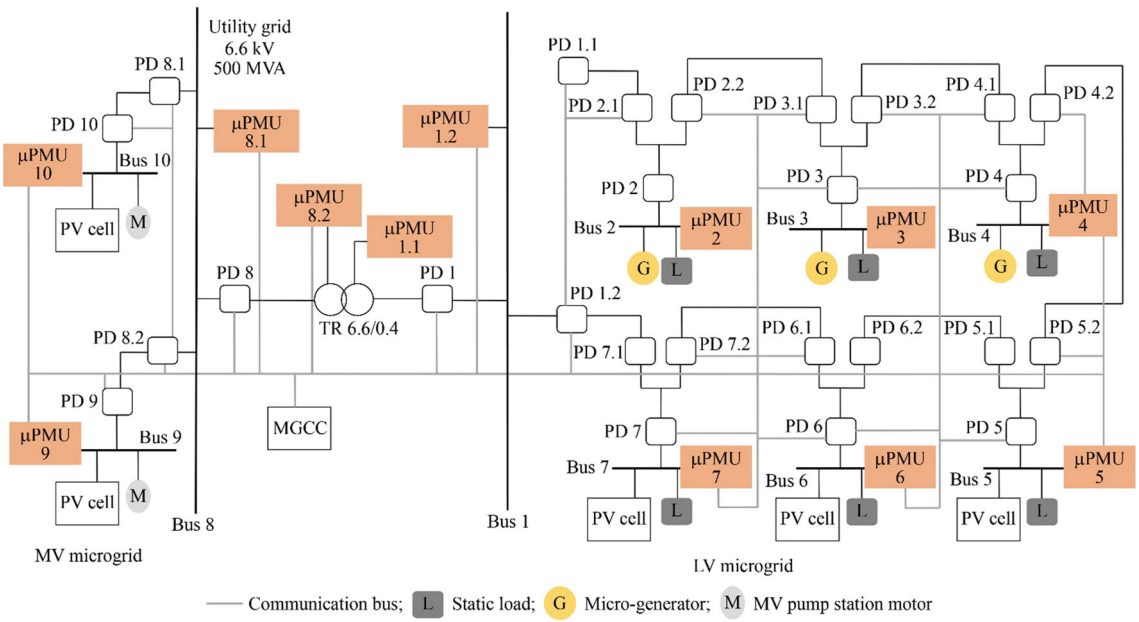

Fig. 3 Single line diagram of MG model

Table 3 µPMU measurement summary of Case 1

Bus	Voltage (V)	Current (A)
1	V_1=396 ∟ −0.3	I_{12}=124 ∟ −27.2
		I_{17}=66 ∟ −25.7
		$I_{TR\text{-}1}$=58 ∟ −27.2
2	V_2=378 ∟ −0.8	I_{21}=124 ∟ −27.2
		I_{23}=30 ∟ −27.2
3	V_3=379 ∟ −0.9	I_{32}=30 ∟ −27.2
		I_{34}=63 ∟ −26.6
4	V_4=382 ∟ −0.6	I_{43}=63 ∟ −26.6
		I_{45}=157 ∟ −26.4
5	V_5=400 ∟ 0	I_{54}=157 ∟ −25.2
6	V_6=400 ∟ 0	–
7	V_7=400 ∟ 0	–
8	V_8=6600 ∟ 0	$I_{8\text{-}TR}$=3.5 ∟ −27.9
9	V_9=6600 ∟ 0	–
10	V_{10}=6600 ∟ 0	–

4.1 Measurement data by µPMUs

This section summarizes the measured data by µPMUs located at each bus for the five cases represented above. Each case has a table summarizing measured data, which are given in the single line diagram with its directional characteristic.

4.1.1 Case 1: normal operation

Load flow is calculated for normal operation. Table 3 and Fig. 4 represent the measured data by µPMUs. Note that in Fig. 4, p.f stands for power factor.

4.1.2 Case 2: grid-connected mode 1

A 3-ϕ Fault is applied on feeder 2-3. Figure 5 represents the measured data by µPMUs. Table 4 shows the µPMU measurement summary of Case 2.

4.1.3 Case 3: grid-connected mode 2

A 3-ϕ fault on feeder 2–3. Figure 6 represents the measured data by MPMUs.

4.1.4 Case 4: three phase fault in islanded mode

A 3-ϕ fault has been applied on feeder 3–4. Table 5 and Fig. 7 represent the measured data, of each bus, by µPMUs.

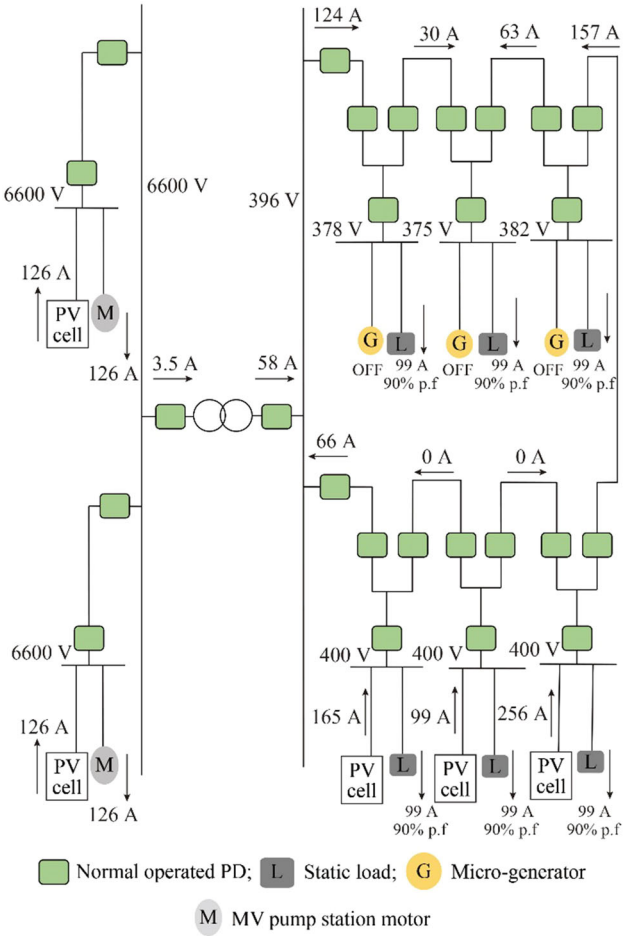

Fig. 4 Directional measurement data of Case 1

4.1.5 Case 5: single phase fault in islanded mode

L-G fault has been applied on feeder 3–4. Table 6 and Fig. 8 represent measured data by µPMUs. µPMU measurements summary of Case 5 are shown in Table 7.

4.2 Protection algorithm evaluation

PD status is identified based on the event and action look-up table. The proposed protection algorithm is tested and evaluated using MATLAB software to detect the fault and abnormality events. Table 8 summarizes the protection algorithm results for each case and the PDs status. It is noticed that the fault detector exists in the faulted feeder and equals to 0 in other feeders. Abnormality detector equals to 1 in simulated fault cases for all buses.

In Case 2, the proposed SPS operates selectively based on the event detection from logic values of D and ∂. The preprogrammed event look-up table in contrast to

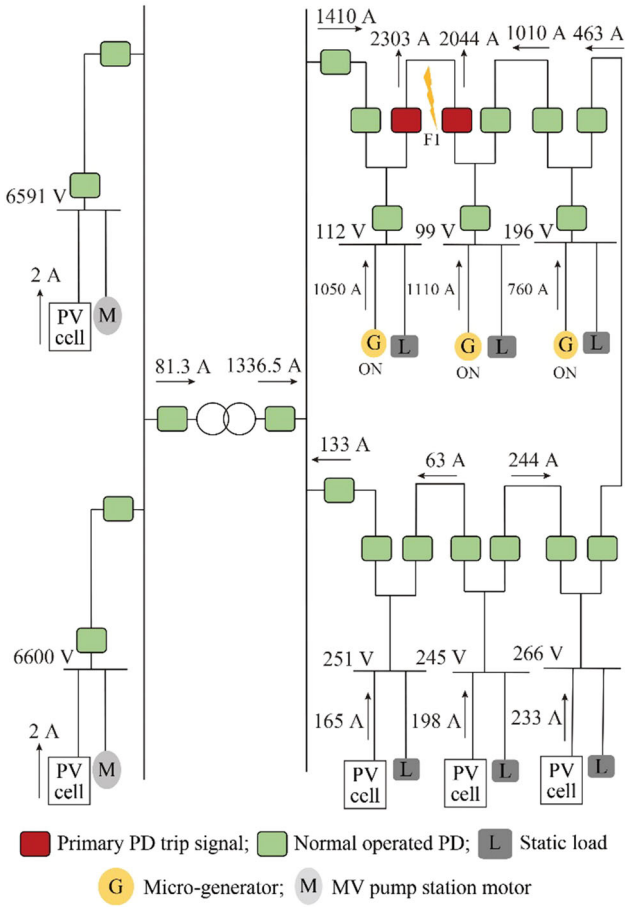

Fig. 5 Directional measurement data of Case 2

conventional overcurrent protection scheme will suffer from sympathic tripping for PDs 1.1, 2.1, 3.2, 4.1, reducing the reliability of the power system.

In Case 3, the proposed SPS operates selectively in contrast to conventional overcurrent protection as PDs 2.2 and 3.1 will suffer from sensitivity issues as fault current laying on long-time tripping of conventional overcurrent relays.

In Case 4, the proposed SPS operates selectively in contrast to conventional overcurrent protection, which will trip generators on buses 2, 3 and 4, causing complete black-out of MG.

In Case 5, the reliability of the proposed SPS in the detection of reduced fault currents is proved to solve all issues related to high impedance faults as well as the

Table 4 μPMU measurement summary of Case 2

Bus	Voltage (V)	Current (A)
1	$V_1 = 246 \angle -1.7$	$I_{12} = 1412 \angle -41.3$
		$I_{71} = 133 \angle 19.4$
		$I_{TR\text{-}1} = 1336 \angle -46.2$
2	$V_2 = 112 \angle -11.3$	$I_{12} = 1412 \angle -41.3$
		$I_{23} = 2303 \angle -58.7$
3	$V_3 = 100 \angle -19.1$	$I_{43} = 1010 \angle -50.8$
		$I_{32} = 2040 \angle -66.6$
4	$V_4 = 196 \angle -11.3$	$I_{43} = 1010 \angle -50.8$
		$I_{54} = 463 \angle -5.58$
5	$V_5 = 226 \angle -2.1$	$I_{54} = 463 \angle -5.58$
		$I_{65} = 244 \angle -13.1$
6	$V_6 = 245 \angle 1.2$	$I_{65} = 244 \angle -13.1$
		$I_{76} = 63 \angle -51$
7	$V_7 = 251 \angle 1.1$	$I_{76} = 63 \angle -51$
		$I_{71} = 133 \angle 19.4$
8	$V_8 = 6590 \angle 29.9$	$I_{8\text{-}TR} = 81 \angle -46.5$
		$I_{9\text{-}8} = 1.4 \angle -4.5$
		$I_{10\text{-}8} = 1.4 \angle -4.5$
9	$V_9 = 6591 \angle 29.9$	$I_{9\text{-}8} = 1.4 \angle -4.5$
10	$V_{10} = 6591 \angle 29.9$	$I_{10\text{-}8} = 1.4 \angle -4.5$

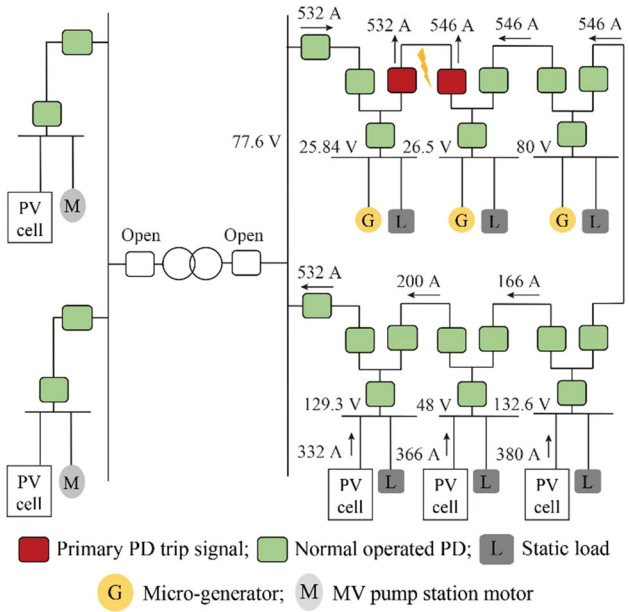

Fig. 6 Directional measurement data of Case 3

Table 5 µPMU measurement summary of Case 3

Bus	Voltage (V)	Current (A)
1	V_1=77.6∟32.8	I_{12}=532∟−14.6
		I_{71}=532∟−14.6
2	V_2=25.84∟32.8	I_{12}=532∟−14.6
		I_{23}=532∟−14.6
3	V_3=26.5∟32.8	I_{43}=546∟−14.6
		I_{32}=546∟−14.6
4	V_4=80∟32.8	I_{43}=546∟−14.6
		I_{54}=546∟−14.6
5	V_5=132.64∟32.8	I_{54}=546∟−14.6
		I_{65}=166∟−16.2
6	V_6=148.72∟32.6	I_{65}=166∟−16.2
		I_{67}=200∟−16.3
7	V_7=129∟32.8	I_{67}=200∟−16.3
		I_{71}=532∟−14.6
8	–	–
9	–	–
10	–	–

Table 6 µPMU measurement summary of Case 4

Measurements	Voltage (V)	Current (A)
1	V_1=145.6∟−26.9	I_{21}=197∟−69.8
		I_{17}=197∟−69.8
2	V_2=164.7∟−26.4	I_{21}=197∟−69.8
		I_{23}=747∟−71.1
3	V_3=92.3∟−28.5	I_{34}=1900∟−76
		I_{23}=747∟−71.1
4	V_4=69.3∟31.9	I_{43}=1430∟−79.3
		I_{54}=197∟−69.8
5	V_5=88.3∟−29.9	I_{54}=197∟−69.8
		I_{65}=197∟−69.8
6	V_6=107.36∟−28.5	I_{65}=197∟−69.8
		I_{76}=197∟−69.8
7	V_7=126.4∟−27.6	I_{76}=197∟−69.8
		I_{17}=197∟−69.8
8	–	–
9	–	–
10	–	–

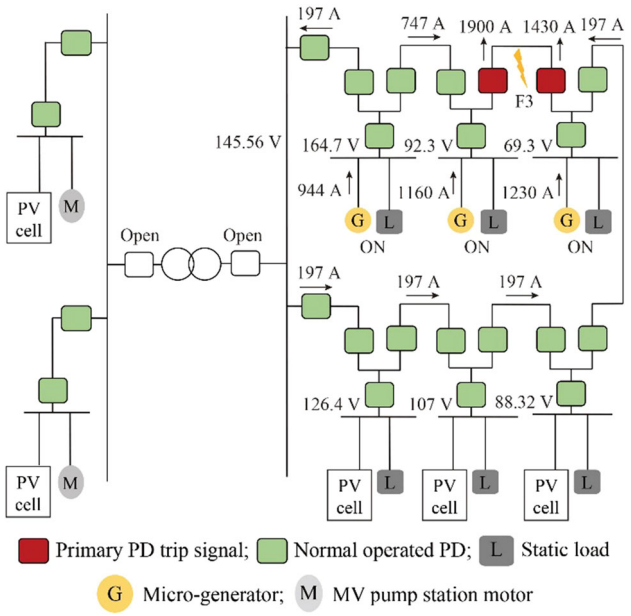

Fig. 7 Directional measurement data of Case 4

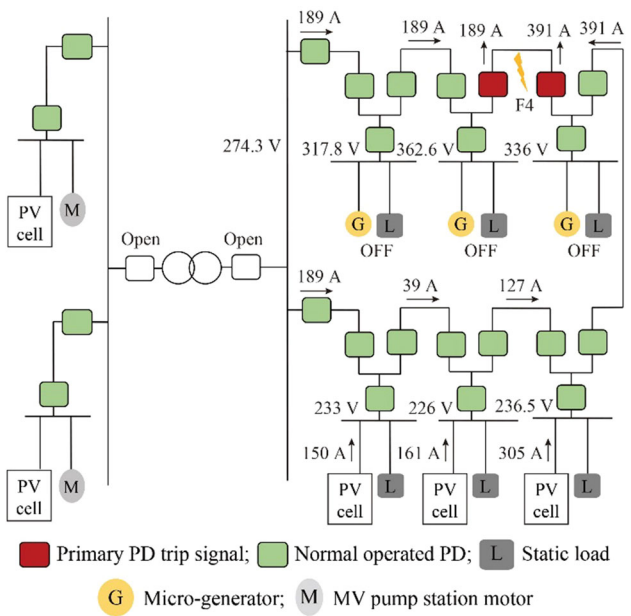

Fig. 8 Directional measurement data of Case 5

islanded mode faults due to high sensitivity of the proposed methods to all faults.

The proposed SPS has the advantage of synchronized data and time tagged measurement which overcomes the problems of measurement overlapping in conventional meter based differential protection and avoids any false tripping. The high accuracy of µPMU estimated phasors can be used for stability assessment and abnormality detection which are not available in differential protection.

In case 5, the fault type can be detected. β component of fault index fails to exist and equals to 0, α components only exist, so the obtained measured phasor can be used to

Table 7 μPMU measurements summary of Case 5

Feeder no.	Sending bus voltage (V)			Feeder current (A)		
	V_a	V_b	V_c	I_a	I_b	I_c
1-2	145.4∟19.8	274.3∟−124.4	232.7∟131.7	199∟−59.9	7∟160.5	7∟160.5
2-3	87.24∟19.8	317.8∟−128.6	249.7∟142.6	199∟−59.9	7∟160.5	7∟160.5
3-F	29.1∟19.8	362.6∟−131.8	274.4∟151.8	199∟−59.9	7∟160.5	7∟160.5
4-F	59∟26.5	335.9∟−131.1	265.5∟146.3	380∟−57.1	7∟−19.5	7∟−19.5
4-5	59∟26.5	335.9∟−131.1	265.5∟146.3	380∟−57.1	7∟−19.5	7∟−19.5
5-6	180∟26.4	236.5∟−124.3	244.14∟123.1	151∟−69.9	33∟166.6	33∟166.6
6-7	214.7∟19.9	224.7∟−117	224.4∟117	24∟−57.8	8∟−72.1	8∟−72.1
7-1	203.6∟19.8	232.85∟−118.6	225.1∟119.7	199∟−59.9	7∟160.5	7∟160.5

Table 8 Results of protection algorithm

Case no.	D_{ij} fault detector	∂_i up normality detector	Event detection	PD status
1	Fail to exist for all buses	∂_i=0 for all buses	Normal operation	All PDs are closed
2	$D_{23}=1$, D_{ij}=0 for all other buses	$\partial_i=1$ for all buses	3-ϕ fault on feeder 2–3	Trip signal to PD 2.2 and PD 3.1
3	$D_{23}=1$, D_{ij}=0 for all other buses	$\partial_i=1$ for all buses	3-ϕ fault on feeder 2–3	Trip signal to PD 2.2 and PD 3.1
4	$D_{34}=1$, D_{ij}=0 for all other buses	$\partial_i=1$ for all buses	3-ϕ fault on feeder 3–4	Trip signal to PD 3.2 and PD 4.1
5	$D_{34}=1$, D_{ij}=0 for all other buses	$\partial_i=1$ for all buses (for over-under voltages)	L-G fault on feeder 3–4	Trip signal to PD 3.2 and PD 4.1

derive zero-positive-negative-sequence components of fault current in the case $I_f=3I_{0,}$ hence (L-G) fault type can be detected. This component analysis is effective for all other (L-L) and (L-L-G) unsymmetrical faults.

5 Conclusion

An SPS is proposed to solve MG protection issues based on a μPMU protection scheme for LV and MV networks. The field tests and simulation results show that the proposed SPS successfully detects and isolates faults in different cases of MG especially when conventional protection schemes are in malfunction. The SPS is proved to be easy programmed with expandable action look-up feature allowing to add any future DGs on the MG. The proposed fault detector and abnormality detector prove to enable quick and accurate fault identification and isolation.

6 Appendix A

Table A1 Grid parameters of MV utility

Parameter of utility grid	Value
Rated voltage (kV)	6.6
Short-circuit power (MVA)	500

Table A2 Load of LV MG

Static loads using DSM	Value
Rated voltage (kV)	0.4
Rated current (A)	100
Rated p.f cos ϕ	0.9

Table A3 Load of MV MG

MV motors used for pump stations	Value
Rated voltage (kV)	6.6
Rated current (A)	126
Rated power (kW)	1250
Speed RPM	1500
No. of poles	4
Rated p.f cos ϕ	0.9258

Table A4 Parameter of LV synchronous DER

Parameter of LV synchronous DER	Value
Rated voltage (kV)	0.4
Rated apparent power/ rated p.f (kVA)	160–0.8
Direct-axis sub-transient reactance X_d (%)	9.6
Quadrature-axis sub-transient reactance X_q (%)	10.2
Direct-axis transient reactance X_d (%)	21
Direct-axis synchronous reactance X_d (%)	260
Negative sequence reactance X_2 (%)	9.8
Zero sequence reactance X_0 (%)	2.1
Direct-axis sub-transient short-circuit time T_d (ms)	11
Direct-axis transient short-circuit time T_d (ms)	85

Table A5 Parameter of LV cable

Parameter of LV cable	Value
Type	XLPE/PVC copper cable, SWA, 1 kV, 50 Hz, 4C
Phase/neutral cross-section (mm^2)	3×240 (3cond./phase)+120
Cable resistance at 90 °C (Ω/km)	0.11031
Cable reactance at 90 °C (Ω/km)	0.08677
Cable length (m)	500

Table A6 Parameter of MV cable

Parameter of MV cable	Value
Type	XLPE/PVC Copper Cable, SWA, 6.6 kV, 50 Hz, 4C
Phase/neutral cross-section (mm^2)	3×300 (5cond./phase)+150
Cable resistance at 90 °C (Ω/km)	0.8068
Cable reactance at 90 °C (Ω/km)	0.07572
Cable length (km)	20

Table A7 Parameter of MV PV cell

Parameter of MV PV cell	Value
Type	Multi-crystalline
Model	PW6-123
No. of cells	36
Panel size (W)	120
Panel max V_{dc} (V)	1000
No. of PV array panels	130 (series), 96 (parallel)
PV array total DC power (kW)	1500
PV array V_{dc} (kV)	2.263
PV array I_{dc} (A)	664

Table A8 Parameter of MV inverter

Parameter of MV inverter	Value
DC ratings	1500 kW, 2500 V, $V_{\max} = 110\%$, $V_{\min} = 0\%$
Efficiency	90% (for different loading conditions)
AC ratings	1350 kVA, 6.6 kV, max p.f = 100%, min p.f = 80%
SC contribution factor	$k = 130\%$
Harmonics (based on IEEE 519)	No. of pulses is 6, shift angle is 0°, Beta is 30°, $X_c = 5\%$, max order is 50

Table A9 LV PV cell specification

Parameters of LV PV cells	Value
Type	Poly-crystalline
Model	YL280P-356
No. of cells	72
Panel size (W)	280
Panel max V_{dc} (V)	1000
No. of PV array panels	20 (series), 39 (parallel)
PV array total DC power (kW)	209
PV array V_{dc} (kV)	688
PV array I_{dc} (A)	303.42

STATE GRID
STATE GRID ELECTRIC POWER RESEARCH INSTITUTE

Table A10 Parameter of LV inverter

Parameter of LV inverter	Value
DC ratings	250 kW, 690 V, V_{max} =110%, V_{min} = 0%
Efficiency	90% (for different load conditions)
AC ratings	225 kVA, 0.4 kV, max p.f is 100%, min p.f is 80%
SC contribution factor	k = 130%
Harmonics (based on IEEE 519 eqn.)	No. of pulses is 6, shift angle is 0°, Beta is 30°, X_c = 5%, max order is 50
Earthing type	TN-S

References

[1] Renewable energy policy network for 21 century Renewables 2016 Global status report (2016) http://www.ren21.net/wp-content/uploads/2016/05/GSR_2016_Full_Report_lowres.pdf. Accessed 15 July 2017
[2] Davies S (2012) Network evolution: developing a modern, intelligent power grid. E&T Mag 7(4):52–55
[3] Hashmi M (2011) Survey of smart grids concepts worldwide. VTT Technical Research Centre of Finland, Finland. http://www.vtt.fi/inf/pdf/workingpapers/2011/W166.pdf Accessed 1 September 2017
[4] Hatziargyriou ND, Anastasiadis AG, Tsikalakis AG et al (2011) Quantification of economic, environmental and operational benefits due to significant penetration of microgrids in a typical LV and MV Greek network. Eur Trans Electr Power 21 (2):1217–1237
[5] Mirsaeidi S, Said DM, Mustafa MW et al (2014) Review and analysis of existing protection strategies for microgrids. Electr Syst 10:1–10
[6] Mirsaeidi S, Said DM, Mustafa MW et al (2014) Progress and problems in micro-grid protection schemes. J Renew Sustain Energy Rev 37:834–839
[7] Choudhary NK, Mohanty SR, Singh RK et al (2014) Protection coordination of overcurrent relays in distribution system with DG and superconducting fault current limiter. In: Proceedings of 18th national power systems conference (NPSC), Guwahati, India, 18–20 December 2014, 5 pp
[8] Imourzadeh ST, Aminifar FO, Anah MD et al (2016) Macro protections for micro grids: toward a new protection paradigm subsequent to distributed energy resource integration. IEEE Ind Electron Mag 10(3):6–18
[9] 1547-2003 -IEEE standard for interconnecting distributed resources with electric power systems (2003) https://ieeexplore.ieee.org/servlet/opac?punumber=8676 Accessed 17 November 2017
[10] Zeineldin HH, El-Saadany EF(2010) Fault current limiters to mitigate recloser fuse miscoordination with distributed generation. In: Proceedings of IET international conference on developments in power system protection, Manchester, UK, 29 March–1 April 2010, 4 pp
[11] Al-Nasseri H, Redfern MA, Li F(2006) A voltage based protection for micro-grids containing power electronic converters. In: Proceedings of 2006 IEEE PES general meeting, Montreal, Canada, 18–22 June 2006, 7 pp
[12] Dewadasa M, Ghosh A, Ledwich G(2011) Protection of microgrids using differential relays. In: Proceedings of 21st Australasian universities power engineering conference (AUPEC), Brisbane, Australia, 25–28 September 2011, 6 pp
[13] Zamani MA, Sidhu TS, Yazdani A (2011) A protection strategy and microprocessor-based relay for low-voltage microgrids. IEEE Trans Power Deliv 26(3):1873–1883
[14] Ahmarinejad A, Hasanpour SM, Babaei M et al (2016) Optimal overcurrent relays coordination in microgrid using Cuckoo algorithm. In: Proceedings of 3rd international conference on power and energy systems engineering, CPESE, Kitaryushu, Japan, 8–10 September 2016, 5 pp
[15] Ragaini E, Oudalov A (2012). Microgrids: building blocks of the smart grid adaptive protection schemes for microgrids. In: Proceedings of 3rd IEEE PES ISGT Europe, Berlin, Germany, 14–17 October 2012
[16] Sarwagya K, Nayak PK (2015) An extensive review on the state-of-art on microgrid protection. In: Proceedings of IEEE power, communication and information technology conference (PCITC), Odisha, India, 15–17 October 2015, pp 862–866
[17] Tsikalakis AG, Hatziargyriou ND (2008) Centralized control for optimizing microgrids operation. IEEE Trans Energy Convers 23(1):241–248
[18] Meier A, Stewart M, McEachern A et al (2017) Precision micro-synchrophasors for distribution systems: a summary of applications. IEEE Trans Smart Grid 8(6):2926–2936
[19] Jain A, Bhullar S (2018) Micro-phasor measurement units (μPMUs) and its applications in smart distribution systems. In: Pillai R et al (eds) ISGW 2017: compendium of technical papers. Lecture notes in electrical engineering, vol 487. Springer, Singapore
[20] Jiang JA, Yang JZ, Lin YH et al (2000) An adaptive PMU based fault detection/location technique for transmission lines part I: theory and algorithms. IEEE Trans Power Deliv 15(2):486–493
[21] Jiang JA, Lin YH, Yang JZ et al (2000) An adaptive PMU based fault detection/location technique for transmission lines—part II: PMU implementation and performance evaluation. IEEE Trans Power Deliv 15(2):1136–1146
[22] IEEE Recommended Practice for the Application of Low-Voltage Circuit Breakers in Industrial and Commercial Power Systems (2015). IEEE standard 3004.5-2014, Feb. https://ieeexplore.ieee.org/servlet/opac?punumber=6856119. Accessed September 2018
[23] Kroposki B, Pink C, Lynch J et al (2007) Development of a high-speed static switch for distributed energy and microgrid applications. In: Proceedings of power conversion conference, Nagoya, Japan 2–5 April 2007 PCC 07, pp 2–5. https://doi.org/10.1109/pccon.2007.373150
[24] Micro-Phasor measurement unit brochure. http://www.powersensorsltd.com/microPMU-brochure.php. Accessed January 2019
[25] Han YQ, Guo CX, Ma S et al (2018) Modeling cascading failures and mitigation strategies in PMU based cyber-physical power systems. J Mod Power Syst Clean Energy 6(5):944–957
[26] Electrical power system analysis and operation software (2016) ETAP software manual. https://etap.com/docs/default-source/whats-new/etap-16-readme.pdf?sfvrsn=10. Accessed 3 November 2017

Mohamed Salah ELBANA obtained the B.Sc. degree in electrical engineering from Faculty of Engineering Alexandria University, Egypt in 2014 with ranking 9th on his colleagues, M.Sc. student at Faculty of Engineering Alexandria University. His researches specialized in enhancing microgrid networks resilience and developments of smart protection and control systems. He worked as teaching assistant at faculty of engineering Alexandria University, Egypt and currently holding position of Senior electrical and instrumentation engineer at Western Desert Petroleum Co. (WEPCO).

Nabil ABBASY obtained the B.Sc., M.Sc. from Alexandria University and Ph.D. from IIT, Chicago, USA in 1988, all in Electrical Engineering. Dr. Abbasy worked at Clarkson University, New York USA and at PAAET, Kuwait. Currently he is an Emeritus Professor at Alexandria University, Egypt. Dr. Abbasy is a senior IEEE member, Editor of IEEE TSG, and A. Editor of MPCE and has authored and coauthored more than 80 papers in the area of power systems monitoring, operation and control.

Ashraf I. MEGAHED received the B.Sc. and M.Sc. degrees in electrical engineering from Alexandria University, Alexandria, Egypt in 1991 and 1994 and the Ph.D. degree from the University of Calgary, Calgary, Canada in 1998. He is currently a Professor at Alexandria University, Egypt. His research interests are digital protection, application of neural networks and wavelet transform in protection.

Nahil SHAKER received the B.Sc. degree in electrical engineering from Alexandria University, Alexandria, Egypt in 2014. She is currently M.Sc. Student in Electrical Engineering department at Alexandria University, Alexandria, Egypt. She is an electrical engineer in "Consulting Engineering Services" company in Alexandria, Egypt. Her research interests are intelligent protection of active distribution network and power system analysis.

STATE GRID
STATE GRID ELECTRIC POWER RESEARCH INSTITUTE